Time- and energy-dependent response of Cs in a strong electric field

F. Robicheaux
Department of Physics, 206 Allison Laboratory, Auburn University, Auburn, Alabama 36849-5311
(Received 9 June 1997)

The results of a theoretical study of Cs atoms in a strong and static electric field are compared to experiment. The atoms are excited from the ground state to $m=0$ or $m=1$ states above the classical ionization threshold. Regularities in the spectra seem to be caused by simple physical mechanisms. The systems are studied in the time domain using two different methods, recurrence spectroscopy and the ejected time dependent flux, and in the energy domain using two different methods, photoionization cross section and expectation values of the energy shift operator. Each of these methods provides some additional insight into the dynamics. [S1050-2947(97)06711-5]

PACS number(s): 32.60.+i, 32.80.Dz, 42.65.Re

I. INTRODUCTION

Studies of the absorption properties of atoms in static electric fields predate the discovery of quantum mechanics. In recent times, the study of alkali-metal atoms in static fields [1–23] has provided several examples of complex dynamics arising from state mixing, avoided crossings, and decay. It is the main purpose of this study to fill in a lightly explored region of the spectrum: above the classical ionization threshold in the field and below the zero field ionization threshold. For this purpose, the energy-dependent photoionization cross section of Cs atoms in 1-kV/cm electric fields has been calculated and compared to experiment [24]. Further, interesting results have been obtained in recent measurements [20,23,25] and calculations [21,22] of the time-dependent flux of electrons that are ejected from the alkali atoms after the atom is exposed to a laser pulse with a duration ~ 4 ps. These two quantities are independent and cannot be obtained from each other. The good agreement that is obtained between the calculated and measured parameters gives confidence that both the theoretical and experimental tools are working well for this system.

In the photoionization measurements, the current of electrons that leaves a gas cell is measured as a function of the frequency of a laser. Because the laser has very high-energy resolution, there is no time-dependent information obtainable from the cross section at a given energy. However, some dynamical information is available by comparing the cross section at several energies. For example, the energy width of a resonance can be related to the state's lifetime and the spacings of energy levels can be related to dynamical periods of the system.

The time information that can be inferred from the cross-section measurements can be *directly* obtained at the expense of energy resolution. Exciting the atom with a pulsed laser generates a superposition of states at several energies. The resulting wave packet evolves in time with features of the wave packet moving in ways reminiscent of classical dynamics. By measuring the time dependence of the flux of electrons ejected from the atom, aspects of the time-dependent electron wave are directly measured. Although some energy resolution is lost in this procedure, there still is a noticeable dependence of the wave-packet dynamics on the main energy of the packet; the dynamics depends on the peak frequency of the laser pulse as well as the pulse's duration.

These two parameters, the photoionization cross section and the time-dependent electron flux, can be used to produce other time-dependent or energy-dependent information. For example, Fourier transforming the energy-dependent cross section gives a quantity that depends on time; this quantity is simply the expectation value of the time translation operator. Fourier transforming the time-dependent electron flux gives a quantity that depends on energy; this quantity is simply the expectation value of an energy translation operator. Each of these Fourier-transformed quantities is a correlation function and thus they may aid in the interpretation of the quantum dynamics. However, it must be kept in mind that the Fourier-transformed quantities are derived parameters and there is no new information that can be gained from them that is not already contained in the cross-section and time-dependent flux.

Alkali-metal atoms in static fields are a fascinating prototype for the behavior of a quantum system with two coupled degrees of freedom. An electron in a pure Coulomb potential and a static electric field has three uncoupled degrees of freedom: φ, ξ, and η where ξ and η are the parabolic coordinates. A hydrogen atom in a static field can be understood in terms of three uncoupled, one-dimensional problems. An alkali atom is much more complicated because the core electrons change the potential for the valence electron from a pure Coulomb potential. This couples together the ξ and η degrees of freedom. Although the coupling between the coordinates may be strong, the coupling is well localized to a small region of space, less than 5 a.u. from the nucleus. This leads to the picture of the electron performing simple uncoupled motion in ξ and η while it is far from the nucleus. But when it returns to the nucleus, the electron may be scattered from one parabolic channel to another.

This possibility qualitatively changes the electron dynamics in the energy range above the classical ionization threshold but below the zero field threshold. In this energy range there will be several channels in parabolic coordinates that are classically open and several channels that are classically closed. The channels arise from the quantization of the motion in the up-field parabolic coordinate. The more energy there is in the upfield coordinate the less there is in the

downfield coordinate. Quantum mechanically, all of the channels are open. However, there is a barrier to escape; this barrier arises from the increasing Coulomb potential energy and decreasing static field potential energy as $z \rightarrow -\infty$. If too much energy is in the upfield motion, the electron must tunnel through this barrier to escape. If very little energy is tied up in the up-field motion, then the electron can travel over the barrier with almost unit probability.

The core electrons qualitatively change the dynamics of the valence electron by scattering it from one parabolic channel to another. The electron is excited into several channels by the photon; some channels are classically open and some are classically closed. For a hydrogen atom, the electron is forced to tunnel out in the closed channels because there is no channel coupling; this causes the resonances in the closed channels to be very sharp. For an alkali atom, the electron does not have to tunnel out if it is in a closed channel because it can scatter from a closed channel to an open channel if it returns to the core. For Cs, the core scatterings are so large that channel coupling, not tunneling, is the dominant decay path of the resonance states.

The dynamics of a Rydberg state of an alkali-metal atom in a static electric field F is governed by two types of motion for small fields. Within an n manifold the Coulomb degeneracy is partially lifted to give states that are nearly equally spaced in energy with a spacing of $3Fn$. The eigenstates are mixtures of many different ℓ states. A wave packet that starts at low ℓ will precess into states with high ℓ before returning to low ℓ states after a time $2\pi/(3Fn)$. The difference in energy between n manifolds is roughly $1/n^3$. Roughly speaking, the time $2\pi/(3Fn)$ may be thought of as the period for an angular-type motion and the time $2\pi n^3$ may be thought of as a radial type of motion. It must be kept in mind that this is not strictly true because the ''angular'' motion is motion in both r and angles. An important observation from our results is that the periodicity, $2\pi/(3Fn)$, remains qualitatively applicable even for n levels and field strengths where perturbation theory breaks down completely.

In Sec. II we discuss the theoretical techniques and the meaning of some of the parameters. In Sec. III, we present results for Cs in a static field.

Atomic units are used throughout this paper unless specified otherwise.

II. THEORETICAL METHODS

This paper presents the results of a study of the energy-dependent and time-dependent response of an alkali-metal atom in a static electric field to a weak laser field. The description of this process rests on correctly calculating the dipole matrix elements connecting the ground state to the final states and on correctly calculating the asymptotic form of the wave function. The theoretical methods used in this paper are the same as those in Refs. [21,22]. We used a modification of Harmin's technique [7,26] for calculating photoionization cross sections in electric fields. In this technique, the wave function near the core is calculated in spherical coordinates. These functions are then transformed into functions of parabolic coordinates, which are appropriate for a particle moving in a constant electric field plus a Coulomb field. These wave functions and the dipole matrix elements that couple them to the initial state are all that is needed to obtain the photoionization cross section and the time-dependent flux of electrons.

As was discussed in Ref. [27], the Fourier transforms of these two quantities may be related to expectation values of translation operators or equivalently to the projection of the initial state onto itself but with every component shifted in energy or time. To be specific, these relationships may be expressed as

$$\begin{aligned}\rho(t) &= \int_{-\infty}^{\infty} R(E)|A(E)|^2 e^{-iEt} dE \\ &= \langle \Psi | U(t) | \Psi \rangle \\ &= \langle \Psi(0) | \Psi(t) \rangle \end{aligned} \tag{1}$$

and

$$\begin{aligned}\eta(\epsilon) &= \frac{1}{2\pi}\int_{-\infty}^{\infty} I(t) e^{-i\epsilon t} dt \\ &= K \int dE \sum_j \langle \psi_g | T | \psi^-_{E+\epsilon,j} \rangle A^*(E+\epsilon) A(E) \\ &\quad \times \langle \psi^-_{Ej} | T | \psi_g \rangle \\ &= \langle \Psi | W(\epsilon) | \Psi \rangle, \end{aligned} \tag{2}$$

where $R(E) = K\Sigma_j |\langle \psi^-_{Ej} | T | \psi_g \rangle|^2$ is the energy-dependent response, T is the transition operator (either z for parallel or x for perpendicular laser polarization), $I(t)$ is the measured time-dependent current, $U(t) = \exp(-iHt)$ is the time translation operator, and

$$W(\varepsilon) = \int dE \sum_j |\psi^-_{E+\varepsilon,j}\rangle\langle\psi^-_{Ej}| \tag{3}$$

is the energy translation operator. The wave function is defined by $|\Psi\rangle = A(H)T|\psi_g\rangle\sqrt{K}$, where H is the Hamiltonian of the system with no laser but with the constant electric field; this function has the energy representation

$$|\Psi\rangle = \sqrt{K}\int dE \sum_j |\psi^-_{Ej}\rangle A(E) \langle \psi^-_{Ej} | T | \psi_g \rangle. \tag{4}$$

The factor $|A(E)|^2$ in Eq. (1) is used to cut off the range of the Fourier transform. $|A(E)|^2$ is chosen to be peaked around a certain energy; the quantity $\rho(t)$ thus depends on the peak energy, the energy width of the $A(E)$ function, and on t. The quantity $\eta(\epsilon)$ depends on ϵ and on the peak of the energy excited by the laser and the laser pulse width.

III. RESULTS

All of the results in this section are for Cs in a constant electric field of 1030 V/cm $= 2.003 \times 10^{-7}$ a.u. The classical ionization threshold is at $E_{\rm th} = -2\sqrt{F} = -8.951 \times 10^{-4}$ a.u. The initial state of the Cs atom is the $6s$ ground state. There are two sequences of results: one for the exciting laser polarized parallel to the constant electric field and the second sequence for perpendicular polarization. In all of the calculations, the spin-orbit interaction is set to zero; this will be a

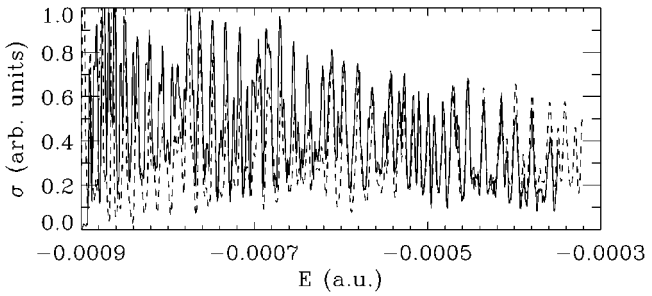

FIG. 1. The experimental (solid line) and calculated (dashed line) photoionization cross section as a function of final-state energy. The laser is polarized parallel to the constant electric field of 1030 V/cm.

good approximation as long as energy scales smaller than 1/2 cm^{-1} or time scales longer than ~ 60 ps are not probed.

Figures 1 and 2 illustrate the measured [24] (solid line) and calculated (dashed line) photoionization cross section as a function of energy of the final state; Fig. 1 is for light polarized parallel to the static field and Fig. 2 is for light polarized perpendicular to the static field. (The cross section is in arbitrary units because I cannot calculate the $6s$ to np dipole matrix element to high accuracy.) The calculated cross section has been convolved with a 0.55 cm^{-1} Gaussian to match the estimated laser resolution. None of the resonances near the classical ionization threshold are resolved. As can be seen from these cross sections, there are a very large number of resonances in this region. The agreement between the calculations and experiments is good considering the number of strongly interacting resonances in this energy region. Overall, the agreement for the perpendicular polarization appears to be somewhat better than for the parallel polarization. This is not too surprising. The coupling between the resonances arises from differences with the Coulomb potential; for $m=0$, there are $\ell=0$, 1, and 2 components that are substantially phase shifted from pure Coulomb waves where as for $m=1$ only $\ell=1$ and 2 are substantially phase shifted; thus any inaccuracy of the calculation will be enhanced for $m=0$. For $m=0$, there is nearly perfect agreement for energies greater than -0.0006 a.u. Below this energy, the positions of the resonances agree but the oscillator strengths do not match up as well. For $m=1$, there is very good agreement over the whole energy range except for a few resonances near -0.0007 a.u.

There are two possible reasons for the descrepencies between the experimental and calculated results. (1) Spin-orbit effects are not negligible. All spin-orbit effects are neglected in the calculation because the amount of p character in the Stark states is relatively small. It may turn out that the cross section is sensitive to the spin-orbit interaction since this interaction mixes eigenstates of the L_z operator. Future work will address this issue. (2) The experimental field strength might not be 1030 V/cm. Small changes in electric field change the oscillator strengths of the resonances. Calculations at several different field strengths did not give results with better agreement; however, it was not possible to do calculations for all possible field strengths and therefore the actual field strength may have been missed.

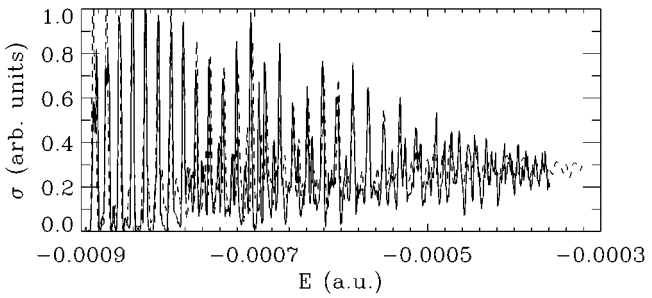

FIG. 2. Same as Fig. 1 but for the laser polarized perpendicular to the constant electric field.

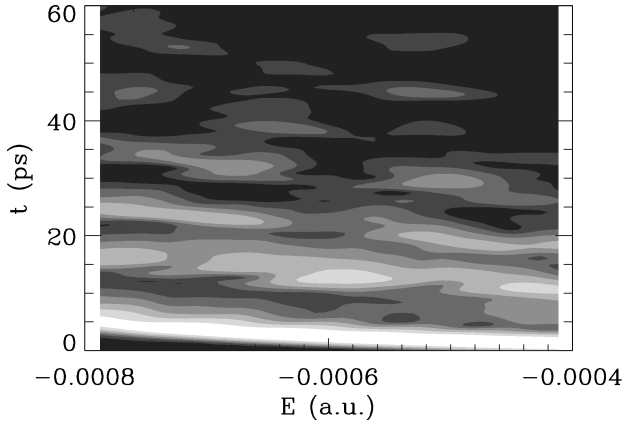

FIG. 3. Contour plot of the electron current ejected from the atom after excitation by a pulsed laser of width 3 ps polarized parallel to the constant electric field. All times have been shifted by a fixed amount. E is the average energy of the packet created by the laser.

We have classified a large number of these resonances. One general trend was that states with roughly the same number of nodes in the up-field and down-field direction (states with small z) were relatively pure states in parabolic coordinates; the states that were localized up-field were strongly mixed in parabolic coordinates. In hindsight, there is a second general trend that is evident in these figures. Near the energies of -0.0008, -0.0006, and -0.0004 a.u. are the energies in H (in a 1030 V/cm field) where levels from the n manifold are nearly degenerate with levels from the $n+1$ manifold. The spectrum near these energies becomes somewhat simple because all states from different manifolds are at the same energy. Near energies of -0.0007 and -0.0005 a.u., the states from adjacent n manifolds are interleaved. The energy spacing of the resonances at these two energies is roughly half that of the resonances near -0.0006 a.u.

In Figs. 3 and 4, the time-dependent electron flux is plotted as contours in E and t. E is the center energy excited by the laser pulse and t is the arrival time shifted by an energy-independent amount. I have compared calculated and measured time-dependent fluxes for this system and obtained very good agreement [21–23]. I only present our calculated results since this was easiest to obtain in a form for contour plotting. The amplitude for the laser to have photons of frequency ω was chosen to be proportional to $\exp[-(E_g+\omega-E)^4/\Gamma^4]$, where $\Gamma=4.8\times10^{-5}$ a.u. This function is somewhat flatter than a Gaussian. With these parameters, the laser has a full width at half maximum of roughly

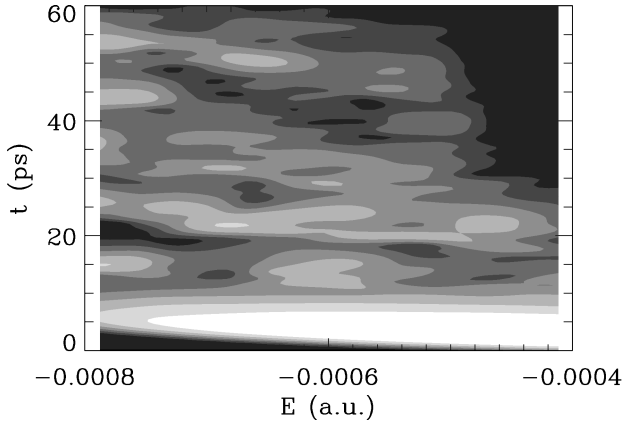

FIG. 4. Same as Fig. 3 but for the laser polarized perpendicular to the constant electric field.

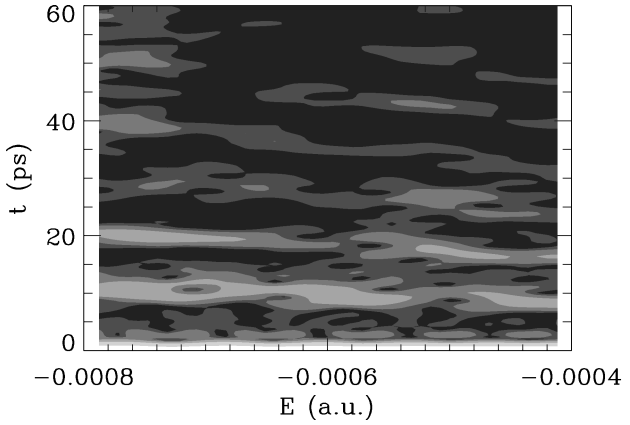

FIG. 5. Contour plot of $|\rho(t)|=|\langle\Psi(0)|\Psi(t)\rangle|$ for a laser polarized parallel to the constant electric field. E is the average energy of the packet created by the laser.

3 ps. This time scale is fast enough to observe the periodicities arising from the $3Fn$ spacing of levels in an n mainifold. But it is not fast enough to observe the periodicities from the $1/n^3$ spacing between manifolds.

There are several features of these graphs that can be understood in a qualitative manner. The white band that starts near 5 ps at $E=-0.0008$ a.u. and ends near 2 ps at $E=-0.0004$ a.u. is from electrons that immediately leave the atom after the laser excitation. The band that starts near 17 ps and finishes near 11 ps arises from the part of the electron wave that is initially in the part of phase space that is closed. But after a time $\tau\sim 2\pi\sqrt{-2E}/(3F)$, the wave packet returns to low angular momentum states and the region near the core. At this point, it can scatter off of the core and part of the wave leaves the atom. The band that starts near 25 ps and finishes near 18 ps comes from the wave packet returning to the core a second time.

Some of the details of these figures have a simple interpretation. The sloping of the bands arises because higher-energy electrons leave the atom faster than lower-energy electrons. The distance of the bands decreases with increasing energy because the time required for the wave packet to evolve from low ℓ to high ℓ then back to low ℓ is $\sim 2\pi\sqrt{-2E}/(3F)$. For $m=1$, the prompt ionization band increases in width with increasing energy; this reflects the fact that more electrons are emitted in the prompt ionization pulse at higher energy. For $m=0$, the prompt ionization band does not change much with energy over this range. The reason for this may be related to an aspect of the classical dynamics. Classically, there is an energy-dependent separatrix angle that divides trajectories starting from the nucleus into bound or escaping trajectories. This separatrix angle is given by [15]

$$\sin(\Theta/2)=-E/\sqrt{4F}. \tag{5}$$

At low energies the separatrix angle is nearly 180°, reflecting the fact that only trajectories launched nearly downfield will leave the atom. As the energy increases, this angle moves to zero, allowing more trajectories to escape. This affects the relative amount that leaves in the direct ionization pulse. At $E=-8\times10^{-4}$ a.u., $\Theta=0.7\pi$, which means for light polarized perpendicular to the field only a very small fraction directly leaves the atom, $\sim 11\%$, because the initial wave has a $\sin^2\theta$ distribution. However, for light polarized parallel to the field roughly half the flux is in the initial pulse, $\sim 40\%$, because the initial outgoing wave has a $\cos^2\theta$ distribution. At $E=-6.33\times10^{-4}$ a.u., $\Theta=\pi/2$, which means half of the initial pulse leaves directly, independent of the polarization. At $E=-4\times10^{-4}$ a.u., $\Theta=0.3\pi$, which means almost all, $\sim 89\%$, of the initial packet directly leaves the atom for perpendicular polarization but still roughly half, $\sim 60\%$, directly leaves for parallel polarization.

Another interesting feature of these figures is the relative size of the first return and second return pulses versus the energy of the packet. At times near -8, -6, and -4×10^{-4} a.u. the first return pulse is maximal. Near -7×10^{-4} and -5×10^{-4} a.u., the second and third return pulses are maximal. This can be related to commensurabilities between spacings of states between n manifolds and between states within n manifolds [23]. This may also be related to the energies of the bifurcations of orbits from the uphill orbit [28].

In Figs. 5 and 6, the magnitude of $\rho(t)$ is plotted as contours in E and t. For this calculation, the same A was used as for the laser excitation in Figs. 3 and 4. Bands similar to those in Figs. 3 and 4 are present in Figs. 5 and 6. This is not too surprising since the necessary condition for flux being ejected is for the wave to return to near the core. These are

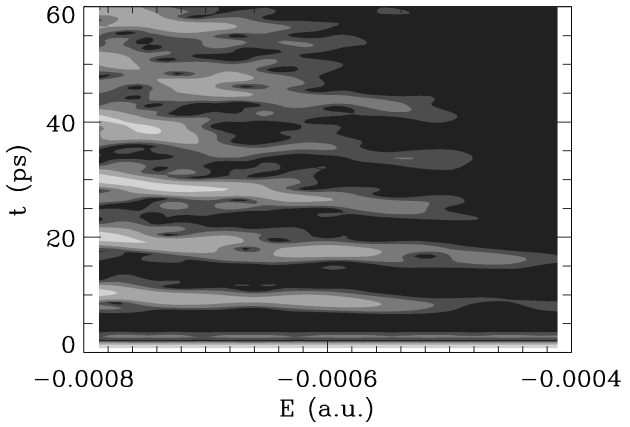

FIG. 6. Same as Fig. 5 but for the laser polarized perpendicular to the constant electric field.

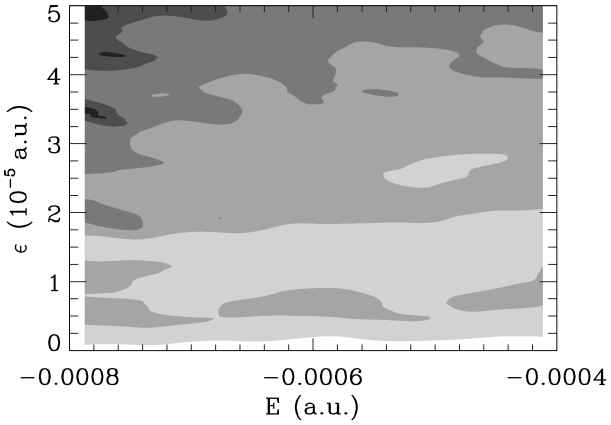

FIG. 7. Contour plot of $|\eta(\epsilon)|$ [$\eta(\epsilon)$ is the expectation value of the energy shift operator] for a laser polarized parallel to the constant electric field. E is the average energy of the packet created by the laser.

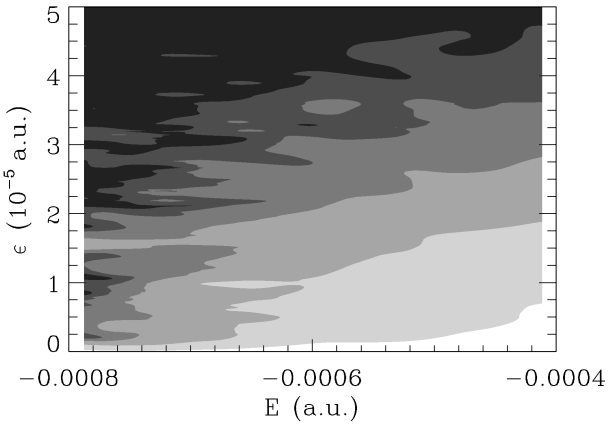

FIG. 8. Same as Fig. 7 but for the laser polarized perpendicular to the constant electric field.

also the times when the overlap of the state at time t with the initial state is maximum. Although there are some similarities between Figs. 3 and 5 and Figs. 4 and 6 a quick comparison shows several major differences. One difference is the initial pulse is fixed at $t=0$; the sloping of the other pulses in Figs. 5 and 6 is strictly due to the periods decreasing with energy. Therefore, no information on the speed that electrons leave the atom is obtainable from $\rho(t)$. The bands in Fig. 6 are much sharper than in Fig. 4 whereas the bands in Fig. 3 are somewhat cleaner than those in Fig. 5. This shows that the same physical mechanism may be observed more easily sometimes using $I(t)$ and sometimes using $\rho(t)$. The same physical mechanism is sometimes expressed in completely different ways between $I(t)$ and $\rho(t)$. For example, the increase of the separatrix angle with energy causes the initial band to broaden in Fig. 4. In Fig. 6, the initial band remains roughly the same width for all energy; however, for E near -0.0004 a.u., there are almost no return overlaps because almost all of the electron wave directly leaves the atom and does not return to the nucleus.

A fourth method for exploring the dynamics is based on the expection value of the energy shift operator, $\eta(\epsilon)$, of Eq. (2). The full information in this parameter is not utilizd in this paper since in Figs. 7 and 8 we only present the contour plot of the absolute value. Most of the information about the general dynamics that is understandable from these figures has already been discussed. However, there is some information that is most simply observed from these figures. Figure 8 *seems* to have relatively little information that is understandable. However, the general upward slope of the contour lines with E is due to the same mechanism that causes the increase of the flux in the first pulse; i.e., the increase of the separatrix angle with energy. This figure gives the clearest indication of this process since it is very close to $E=-6.3\times10^{-4}$ a.u. that the second contour line increases most rapidly. In Fig. 7, the band near $\epsilon=1.5\times10^{-5}$ a.u. arises from the first return of the wave packet to the nucleus. The band near $\epsilon=0.75\times10^{-5}$ a.u. arises from the second return. It is interesting that only near energies $E=-7\times10^{-4}$ and -5×10^{-4} a.u. are the second returns strong. There is almost no sign of a second return pulse near $E=-8\times10^{-4}$ a.u.; i.e. there is not a peak near $\epsilon=0.75\times10^{-5}$ a.u. at this energy. This is a clear indication of the mechanism that causes the second return pulses: near energies $E=-7\times10^{-4}$ and -5×10^{-4} a.u. the second return pulse in Figs. 3 and 5 is strong because the energies have a spacing half that of the expected spacing but near energy $E=-8\times10^{-4}$ a.u. the second return pulse in Figs. 3 and 5 is strong because the resonances have a long lifetime and it takes multiple return to the core for the wave packet to fully decay. There is one feature in Fig. 7 that does not have a clear counterpart in the other figures. This is the peak in the energy translation operator for $E=-5\times10^{-4}$ a.u. and $\epsilon=2.6\times10^{-4}$ a.u. This peak implies some sort of time dependent process with a period roughly 3/5 that of the main period. A simple physical reason for this peak is not known at this time.

IV. SUMMARY

We have explored the dynamics of Cs in a strong electric field. Contrary to simple expectations, we have found that the dynamics is dominated by the simple periodicities that are present in the ℓ-mixing regime. Some effects from n mixing affect the character of the dynamics at longer times. By investigating the dynamics using four different methods, we have found that simple mechanisms control the behavior of the parameters that we have plotted and thus a coarse level of understanding is possible in this system with many interacting levels.

The parameter that seemed to give the most information on the coarse level dynamics was the time-dependent current of electrons measured as a function of the central energy of the laser pulse. The recurrence spectrum (which is obtained from the photoionization cross section) gave nearly the same level of information but could not give any information about how the electron leaves the atom.

ACKNOWLEDGMENTS

F.R. was supported by the NSF. I thank G. M. Lankhuijzen and L. D. Noordam for providing unpublished experimental data.

[1] M.G. Littman, M.L. Zimmerman, T.W. Ducas, R.R. Freeman, and D. Kleppner, Phys. Rev. Lett. **36**, 14 (1976).
[2] R.R. Freeman, N.P. Economu, G.C. Bjorkland, and K.T. Lu, Phys. Rev. Lett. **41**, 1463 (1978).
[3] R.R. Freeman and N.P. Economu, Phys. Rev. A **20**, 2356 (1979).
[4] M.L. Zimmerman, M.G. Littman, M.M. Kash, and D. Kleppner, Phys. Rev. A **20**, 2251 (1979).
[5] P.M. Koch and D.R. Mariani, Phys. Rev. Lett. **46**, 1275 (1981).
[6] T.S. Luk, L. DiMauro, T. Bergeman, and H. Metcalf, Phys. Rev. Lett. **47**, 83 (1981).
[7] D.A. Harmin, Phys. Rev. A **24**, 2491 (1981); **26**, 2656 (1982).
[8] S. Feneuille, S. Liberman, E. Luc-Koenig, J. Pinard, and A. Taleb, J. Phys. B **15**, 1205 (1982).
[9] U. Eichmann, K. Richter, D. Wintgen, and W. Sandner, Phys. Rev. Lett. **61**, 2438 (1988).
[10] A. Nussenzweig, E. Eyler, T. Bergeman, and E. Pollack, Phys. Rev. A **41**, 4944 (1990).
[11] M.H. Halley, D. Delande, and K.T. Taylor, J. Phys. B **25**, L525 (1992).
[12] D.J. Armstrong, C.H. Greene, R.P. Wood, and J. Cooper, Phys. Rev. Lett. **70**, 2379 (1993).
[13] B. Broers, J.F. Christian, J.H. Hoogenraad, W.J. van der Zande, H.B. van Linden van den Heuvell, and L.D. Noordam, Phys. Rev. Lett. **71**, 344 (1993); B. Broers, J.F. Christian, and H.B. van Linden van den Heuvell, Phys. Rev. A **49**, 2498 (1994).
[14] I. Seipp and K.T. Taylor, J. Phys. B **27**, 2785 (1994).
[15] J. Gao and J.B. Delos, Phys. Rev. A **49**, 869 (1994).
[16] M. Courtney, N. Spellmeyer, H. Jiao, D. Kleppner, J. Gao, and J.B. Delos, Phys. Rev. Lett. **74**, 1538 (1995).
[17] G.M. Lankhuijzen and L.D. Noordam, Phys. Rev. A **52**, 2016 (1995).
[18] G.J. Kuik, A. Kips, W. Vassen, and W. Hogervorst, J. Phys. B **29**, 2159 (1996).
[19] G.D. Stevens, C.-H. Iu, T. Bergeman, H.J. Metcalf, I. Seipp, K.T. Taylor, and D. Delande, Phys. Rev. A **53**, 1349 (1996).
[20] G.M. Lankhuijzen and L.D. Noordam, Phys. Rev. Lett. **76**, 1784 (1996).
[21] F. Robicheaux and J. Shaw, Phys. Rev. Lett. **77**, 4154 (1996).
[22] F. Robicheaux and J. Shaw, Phys. Rev. A **56**, 278 (1997).
[23] G.M. Lankhuijzen, F. Robicheaux, and L. D. Noordam, Phys. Rev. Lett. **79**, 2427 (1997).
[24] G. M. Lankhuijzen and L. D. Noordam (unpublished).
[25] G. M. Lankhuijzen and L. D. Noordam, Opt. Commun. **129**, 361 (1996).
[26] U. Fano, Phys. Rev. A **24**, 619 (1981).
[27] F. Robicheaux, Phys. Rev. A **56**, 4296 (1997).
[28] J. Wals and H.B. van Linden van den Heuvell, J. Phys. B **30**, 941 (1997).